J. Phys. D: Appl. Phys. **33** (2000) 1985–1989. Printed in the UK PII: S0022-3727(00)11451-2

Mössbauer studies of Fe–Si–C system structure changes by laser and ultrasound treatment

A Amulevicius, K Mazeika and A Daugvila

Institute of Physics, A Gostauto 12, 2600 Vilnius, Lithuania

Received 31 January 2000, in final form 23 May 2000

Abstract. The influence of simultaneous laser irradiation and ultrasound on the phase structure of the Fe–Si–C system (grey cast iron) was studied by means of Mössbauer spectroscopy. It has been found that the efficiency of the ultrasound influence depends on the melted layer depth (temperature). Ultrasound affects the phase structure of the melted volume, though in the surface layer, which is of the highest temperature, it does not alter the amount of martensite and iron carbide. The major effects of ultrasound are assistance in dissolving carbon and in disintegrating oversaturated γ–Fe(C) solution. It is shown that structures similar to the structure of the solid Fe(C) system should originate in the melted state.

1. Introduction

Physical–chemical properties of alloys depend on the atomic ordering, the dispersion structure of the material, the composition and equilibrium of phases. For the modification of alloy properties, it is expedient to apply laser irradiation. It enables a change in the duration of the melt state and the cooling rate by means of varying the power and duration of irradiation [1–3]. The application of laser irradiation allows the modification of the alloy dispersion and the fixing of the atomic ordering and the structure of a solid state that is characteristic of a liquid state before solidification.

The application of additional external factors influencing the sample structure may help in a better understanding of the processes taking place in the melt during laser irradiation. Acoustic methods were used to study the effects of the short-range chemical ordering and reordering of the atomic structure, which was influenced by diffusion of impurities and defects of the structure, as well as to study the dislocation structures and crystallization [4, 5]. It must be noted that processes of crystallization are of the utmost importance to the properties of the alloys. The high-capacity ultrasound equipment is widely used to affect the crystallization but only under quasi-stationary conditions. There are few studies on the crystallization from the melt state of a millisecond duration. In [6], laser irradiation and ultrasound were used for the implantation of the surface layer of steel.

The aim of this work is an attempt to study the effects of ultrasound on the phase formation of the alloy from the melt of a short duration at a high quenching rate and to determine the major processes of the phase formation.

In this work, an acoustic concentrator of a special design [7] was used to affect the melt structure obtained by simultaneous laser irradiation of a duration of $\approx$0.1 s.

2. Experimental conditions

The alloy Fe–Si–C (grey cast iron) was investigated. The x-ray chemical analysis has shown that the alloy contains 2.78 at.% of Si, 0.3 at.% of Cr, 1.2 at.% of Mn and about 14.5 at.% of C. The microscopic studies revealed that carbon existed as the graphite insertions in the layered structure with the distance of some micrometres between the graphite layers. The structure of grey cast iron is favourable for the research because, differing from laser implantation [8], carbon does not evaporate from the surface and mixes with iron successfully. A small amount of other impurities in grey cast iron allows the successful study of the formation of the phases of martensite, iron carbides and retained austenite on the basis of this system.

The Mössbauer studies were carried out with the constant acceleration spectrometer in transmission geometry at room temperature. The statistics for the spectrum point were $>10^6$. The samples were processed with the CO_2 laser equipment of continuous action with the power of 800 W. The wavelength of the laser was 10.6 μm. The laser beam was focused on a spot of the $d \leqslant$ 1–1.5 mm diameter. The scanning velocity of 10 mm s^{-1} determined the duration of the sample irradiation by the laser beam of $\approx$0.1 s. Scans were repeated across the sample surface with less than 25% overlaps. Due to this processing, the surface layer of $\approx$200 μm thickness was melted.

The application of conversion electron Mössbauer spectroscopy (CEMS) enables the study of the layer up to the 0.02 μm depth, therefore it is effective only for the studies of the surface layer that is influenced by laser irradiation of a nanosecond duration. In our studies, the surface that was treated with laser irradiation and ultrasound was abraded and the powder from the desirable depth was used to prepare the samples for the Mössbauer studies. The samples were

0022-3727/00/161985+05$30.00 © 2000 IOP Publishing Ltd

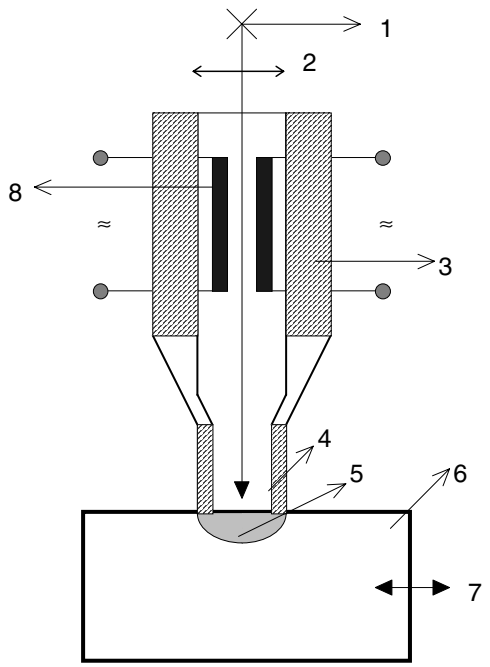

Figure 1. A schematic diagram of the simultaneous processing of the sample surface by laser irradiation and ultrasound: 1, laser beam; 2, lens; 3, converter; 4, waveguide-concentrator; 5, melted region; 6, sample; 7, the direction of the scan; 8, excitation reels.

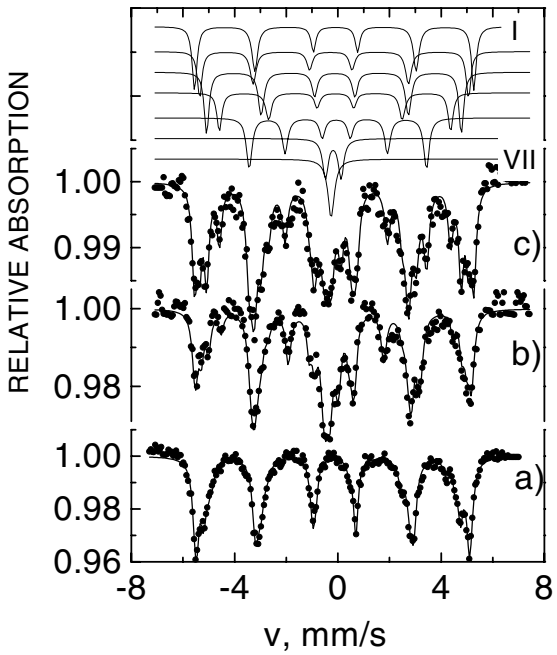

Figure 2. Mössbauer spectra and the corresponding subspectra from the least-squares fit for initial grey cast iron: (a) for samples taken from the surface ($h = 0$–20 μm) only after laser irradiation; (b) after the simultaneous impact of laser irradiation and ultrasound at $P = P_{max}$ (c). The subspectra I–III correspond to martensite, IV to iron–carbon clusters, V to iron carbide, and VI–VII are subspectra of austenite.

abraded in kerosene to prevent the heating and the possible changes in physical–chemical properties. The samples for the Mössbauer studies were obtained from the depths h: 0–20, 150–170, 210–230, 310–330 and 410–430 μm. The thickness of the samples was 20 mg cm^{-2} of natural iron.

The combined treatment of laser irradiation and ultrasound was carried out by the use of the ultrasound device of special design (figure 1). The appliance of a lens allowed us to locate the ultrasound converter and the concentrator coaxially to the laser beam. The dimension of the processed samples was $30 \times 30 \times 10$ mm^3. The frequency of the ultrasound waves was chosen to be 44 kHz. The impact of ultrasound was concentrated in the zone of laser irradiation by means of the waveguide-concentrator which was pressed to the sample surface with the power of 13 N and the contact area of 2 mm^2. The electrical power of the acoustic converter reached 40 W. Due to difficulties in determining quantitatively the absorbed power of ultrasound in the melted volume, for the description of the results we chose relative values of the ultrasound power normalized to the maximum power P_{max}. The samples for the Mössbauer studies were taken from the area of 20×20 mm^2 to average the inhomogeneity of the material.

The temperature in the regions melted by laser irradiation was obtained by numerically solving the heat conduction equation. The calculations allowed us to include the heat of melting and evaporation, temperature dependences of the density, of the specific heat and of the heat conductivity (for more details see [9]). They allowed us to evaluate and to compare the temperatures at different depths. The surface layer ($h = 0$–20 μm) had the highest temperature, 2500 K. The deeper layers had the following temperatures: $h = 150$–170 μm, 2000 K; $h = 210$–230 μm, 1700 K; $h = 310$–330 μm, 1500 K; $h = 410$–430 μm, 1400 K. The bath of the melt had a volume of 0.2–0.3 mm^3. After laser irradiation, the bath quenched to room temperature with the rate of 10^4–10^5 K s^{-1} and the phase transition γ-Fe–α-Fe had the features of martensite.

The obtained Mössbauer spectra were fitted to the sum of subspectra of austenite, martensite, iron–carbon clusters, cementite (Fe_3C) by the least-squares procedure (figure 2). The spectra of martensite were resolved into subspectra corresponding to various arrangements of impurity atoms around Fe atoms. The hyperfine magnetic field at the nuclei of Fe atoms for these arrangements was described in the additive approximation [10, 11]

$$H(m,n) = H^{Fe} - m\Delta H_1 - n\Delta H_2 + \Delta H(0,0) \quad (1)$$

where m and n are the number of impurity atoms in the first and second coordination shells (cs) of iron, H^{Fe} is the magnetic field in pure iron, and ΔH_1 and ΔH_2 are field shifts due to the presence of impurity atoms in I and II cs, respectively. Magnetic field shifts are approximately equal for both substitutional impurities (Si, Mn, Cr) and interstitial carbon, $\Delta H_1 \approx 2.7$ T and $\Delta H_2 \approx 1.3$ T [10, 12].

For the description of spectra, three subspectra of martensite were taken for Fe atom environments with (0,0), (0,1) and (1,0) impurity atoms in I and II cs, respectively. The probabilities of these iron environments or the relative area of subspectra P_1, P_2 and P_3 may be found as

$$P_1 = P_P^M(0,0)P_C^M(0,0) \quad (2a)$$
$$P_2 = P_P^M(0,1) + P_C^M(0,1) \quad (2b)$$
$$P_3 = P_P^M(1,0) + P_C^M(1,0) \quad (2c)$$

with a good approximation. $P_{\mathrm{P}}^{\mathrm{M}}(m,n)$ and $P_{\mathrm{C}}^{\mathrm{M}}(m,n)$ are the probabilities of the Fe environment for substitutional impurity and interstitial carbon, respectively. The probabilities may be calculated on the basis of binomial distribution.

The value of the effective magnetic field at the Fe nuclei of atoms, which have no impurities in the first two coordination spheres H_{eff} (0,0), can be evaluated from the largest magnetic splitting of subspectra of martensite. According to [11, 13, 14], H_{eff} (0,0) can be expressed by the percentage of impurities:

$$H_{\mathrm{eff}}(0,0) = H^{\mathrm{Fe}} + 0.13c_{\mathrm{C}}^{\mathrm{M}} + 0.1c_{\mathrm{P}}^{\mathrm{M}} \qquad (3)$$

where the magnetic field is expressed in Tesla (T), $c_{\mathrm{C}}^{\mathrm{M}}$ is the atomic percentage of carbon, and $c_{\mathrm{P}}^{\mathrm{M}}$ is the atomic percentage of substitutional impurities in martensite.

For a description of austenite, the single peak and the quadrupole doublet were used. These are attributed to iron atoms with no carbon, and iron atoms with one carbon in I cs. The isomer shift was 0.05 mm s^{-1} for the single peak and 0.08 mm s^{-1} for the doublet. Quadrupole splitting was 0.6 mm s^{-1}.

An additional sextet with the corresponding hyperfine magnetic field $H \approx 20.8$ T was used to describe cementite. The detection in Mössbauer spectra of other ε and χ iron carbides, which have three different environments of iron, was carried out in the regions of magnetic fields within 17–19 T, 22–23.4 T and 11–13 T.

The iron–carbon clusters were described by the sextet with the magnetic field 26–28 T. Due to a very small amount of ε and χ carbides, Mössbauer spectra were fitted to the sum of seven subspectra: three of martensite, two of austenite, one of iron–carbon clusters, and one of cementite.

The atomic percentage of the substitutional impurities and carbon in martensite may be evaluated on the basis of equations (2*a*), (2*b*), (2*c*) and (3). Accordingly, the atomic percentage of carbon in austenite $c_{\mathrm{C}}^{\mathrm{A}}$ was determined on the basis of the probability of binomial distribution for iron which has no carbon atoms in I and II cs:

$$P_{\mathrm{A}}(0) = \left(1 - c_{\mathrm{C}}^{\mathrm{A}}\right)^6. \qquad (4)$$

3. Results

According to our recent publication [2] and this work, the qualitative changes in phase composition obtained after laser irradiation of grey cast iron are reflected in figure 3. The application of ultrasound causes additional changes. In the surface layer (h = 0–20 μm), the ultrasound influence is reflected by the amount of two phases—austenite and iron–carbon clusters—but in a deeper layer (h = 150–170 μm) the influence is seen in redistribution of all phases. The Mössbauer spectra of the characteristic samples and their fit are shown in figure 2 and the percentage of constituent phases of the samples, in figures 4(a) and (b).

The analysis of the Mössbauer spectra has shown that primary grey cast iron consists of ferrite, for which there are subspectra representing the substitutional impurity atoms in I and II cs. The common Si, Mn and Cr atomic percentage of ≈4 at.% was found on the basis of equation (3).

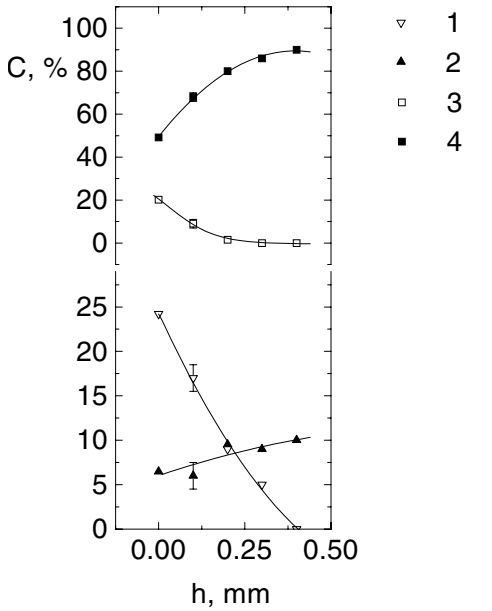

Figure 3. The depth dependence on the phase structure of initial grey cast iron treated with laser irradiation of 0.1 s duration: 1, austenite; 2, iron–carbon clusters; 3, iron carbide; 4, martensite.

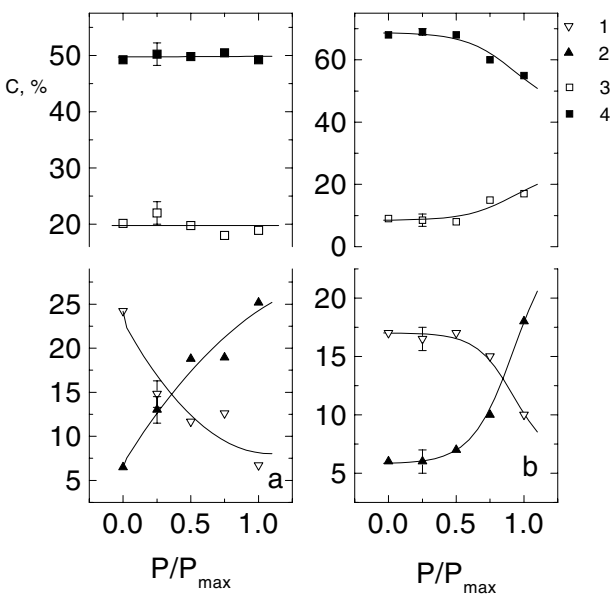

Figure 4. The ultrasound relative power $P/P_{\max}$ dependences on the phase structure of samples treated with laser irradiation of 0.1 s duration taken at the depths, (a) h = 0–20 μm and (b) h = 150–170 μm: 1, austenite; 2, iron–carbon clusters; 3, iron carbide; 4, martensite.

During the experiments, the conditions of laser irradiation were invariable. Laser irradiation causes large phase changes in the composition of the samples. On the surface, after laser irradiation, the amount of phases reached 24% for retained austenite, 20% for iron carbide, 6% for iron–carbon clusters and 50% for martensite (figure 3). On the basis of equations (2*a*), (2*b*), (2*c*) and (3), the atomic percentage of carbon in martensite was found to be 3–4 at.%.

For the surface layer, figure 4(a) shows that the amount of martensite and iron carbide does not depend on the

ultrasound power. The amount of austenite decreases and the amount of iron–carbon clusters increases proportionally with the increase in the ultrasound power. Approximately the common atomic percentage of both phases remains stable and amounts to about 30 at.%.

In the sample taken from a deeper layer (150–170 μm), the phase structure dependence is more complicated (figure 4(b)). The composition of the samples is almost invariable up to a certain level of the ultrasound power (0.5 P_{max}). The power increase above this level causes a decrease in the amount of martensite and austenite as well as an increase in the amount of iron carbide and iron–carbon clusters. At the depth h = 210–230 μm, the influence of ultrasound was not detected, though all four phases were formed by laser irradiation. The samples taken from the depth h = 310–330 μm do not reveal the influence of either laser irradiation or ultrasound.

4. Discussion

The steep temperature gradient in the liquid bath causes convective streams that, together with diffusion, redistribute carbon in the melt. The coefficients of diffusion $D(T)$ at different temperatures in the melt are related to the viscosity: $D(T_2)/D(T_1) = (T_2/T_1)(\eta(T_1)/\eta(T2))$, where $\eta(T_1)$ and $\eta(T_2)$ are viscosities of the melt at temperatures T_1, T_2. In our case, this relation for the surface and deeper layers (150–170 μm) is about 4 [15].

The viscosity of the melted metal depends on temperature exponentially [16] $\eta(T) \sim \exp(E/kT)$ where E is the activation energy and k is the Boltzmann constant. The absorption of ultrasound is proportional to viscosity, but in our system the viscosity strongly depends on the structure heterogeneity—the insertion of solid phases (graphite, iron carbide) into the melt. Therefore, it can be much larger than the viscosity of the pure liquid metal at the same temperature. In the case of spherical insertions [16], the viscosity increases as

$$\frac{\eta_e}{\eta_i} = 1 + 2.5\varphi + 7\varphi^2 + \ldots \qquad (5)$$

where η_e is the real viscosity and η_i is the viscosity without solid insertions of the relative volume φ. Moreover, ultrasound helps not only to distribute atoms in the melt, but also takes part in the formation of embryos of phases [17].

The duration of 0.1 s of the melted state is not sufficient to reach the equilibrium distribution of carbon. Where the carbon concentration is high enough already at temperatures higher than the melt temperature of grey cast iron, particles of carbide Fe_3C form in the melt. Excluding the carbide phase, still 9.5 at.% of carbon remains in the rest of the melt. The martensite has 3–4 at.% of carbon. As the martensite forms after indiffusive transition, the region with the same concentration of carbon should also exist in the melt.

Because of the high temperature in the surface layer, the thermal motion covers the influence of ultrasound for dissolving and mixing carbon. Due to the lack of efficiency of the ultrasound influence, the amount of iron carbide and martensite remains stable. Excluding the carbide and martensite in the residue which has 30% of iron, the average atomic percentage of carbon makes up about 24 at.%, that is twice the solubility limit of 10.5 at.% in γ-Fe [18]. By means of Mössbauer spectroscopy it was found that the atomic percentage in γ-Fe was close to the solubility limit and was about 9.5 at.%.

After excluding the phases of martensite, iron carbide, austenite and their amount of carbon, we obtained the average composition of the residue (table 1). On the basis of these results, we can discuss the amount of carbon in iron–carbon clusters. Although the obtained composition of the residue is close to the composition of ε-$Fe_{2.4}C$, χ-Fe_5C_2 and θ-Fe_3C carbides, the corresponding area of subspectra of ε and χ carbides in the fit of all Mössbauer spectra is small within experimental errors. In the spectra, only the subspectra with the effective fields H_{eff} close to 20.8 and 27–29 T were found with the sufficient resolution. The first value corresponds to the θ-Fe_3C carbide and the second is attributed to iron atoms with two carbon atoms in I cs and/or iron–carbon clusters [19]. According to the binomial distribution, the probability that iron will have two carbon atoms in I cs is small and a major part of the 27–29 T subspectrum is associated with iron–carbon clusters. The clusters are described by one subspectrum, therefore their atomic structure and the amount of carbon in all samples should remain approximately invariable. According to table 1, at the maximum ultrasound power the highest limit to the amount of carbon in the clusters must be about 30 at.% considering that all graphite is dissolved. Evidently at the lower ultrasound power, some carbon should be assumed not to be dissolved. In the case of the 30 at.% percentage of carbon in iron–carbon clusters in the surface layer, at least 23% of all carbon remains as graphite, when the sample is treated only by laser irradiation. For the deeper layers, the phases of iron contain less carbon, and the content of graphite is still larger. Evidently, ultrasound helps to dissolve carbon and influences its distribution in the melt.

Table 1. Atomic percentage of carbon in the iron–carbon clusters and residual graphite (Fe, 100%) and the corresponding average chemical forms regarding phases as a common solid solution.

	h = 0–20 μm		h = 150–170 μm	
P/P_{max}	c_C at.%	Form	c_C at.%	Form
0	82.3	$Fe_{1.2}C$	136.2	$FeC_{1.4}$
0.25	44.3	$Fe_{2.3}C$	138.5	$FeC_{1.4}$
0.5	35.4	$Fe_{2.8}C$	120.3	$FeC_{1.2}$
0.75	36.8	$Fe_{2.7}C$	71.5	$Fe_{1.4}C$
1.0	29.3	$Fe_{3.4}C$	40.7	$Fe_{2.5}C$

Let us determine in which state, liquid or solid, of the melt the redistribution of the Fe–C solution in the γ-Fe(C) and the iron–carbon clusters takes place. In this case, the analysis of the phase structure of the samples taken from a deeper layer (h = 150–170 μm) (figure 4(b)) can help. In a deeper layer, ultrasound starts to influence the phase structure only at the power $P > 0.5P_{max}$. Due to the larger viscosity related to the lower temperature, the diffusive and convective processes become weaker and a relative influence of ultrasound increases. In a deeper layer of the melt, ultrasound helps to mix atoms of carbon with iron and to originate new embryos of grains, that reflect an increase in the amount of iron carbide and a proportional decrease in the

amount of free iron (figure 4(b)). In this study, the applied ultrasound power was not sufficient for the $h = 150$–$170\ \mu$m layer to reach the solubility of carbon and the amount of iron–carbon phases characteristic of the surface layer.

It may be assumed that the redistribution of oversaturated solution into austenite and clusters takes place during the martensite phase transition, i.e., in the solid state. It may be stimulated by the metastability of the oversaturated solution and the deformation of austenite, which occur during the martensite phase transition [20]. If such redistribution takes place in a solid state, the existence of a threshold for the deeper layer cannot be explained.

While the melt quenches, and the viscosity and the absorption of ultrasound increase, the redistribution of the oversaturated solution Fe–C is stimulated. One part of the melt with the carbon amount close to the solubility limit forms γ-Fe and in the other part the clusters are built. Due to the influence of laser irradiation at high cooling rates, the high dispersity structure is formed [21]. The energy related to the crystal grain interface becomes large, and the interfacial layer is needed to reduce the energy of intergranular tensions [22]. The iron–carbon clusters are assumed to be mainly the accumulation of the chaotic-ordered elementary cells [23] which probably have the structure associated with neighbouring grains and are located in the boundary region.

Referring to the results, we propose the sequence of processes when laser irradiation and ultrasound affect grey cast iron. After heating and dissolving carbon in the melted layer at a temperature higher than the melt temperature of grey cast iron, the iron carbide phase cystallizes out into the melt in the regions enriched with carbon of sufficient concentration. Because of the non-equilibrium distribution of carbon, the melt γ-Fe(C) has highly enriched and depleted regions of carbon. With a certain absorbed power of ultrasound, the disintegration of the oversaturated Fe–C into austenite and iron–carbon clusters takes place. These regions with a different percentage of carbon and structures similar to those of iron carbide, austenite and iron–carbon clusters are formed before the transition to solid state of the melt [16].

5. Conclusions

(1) The application of ultrasound allows us to reduce the amount of retained austenite in the samples by 2–3 times. The decrease in γ-Fe takes place mainly due to the distribution of carbon between austenite and iron–carbon clusters.
(2) The threshold of the influence of ultrasound on the structure of the melt was observed. In liquid phase, the threshold is defined by the viscosity of the melt and the absorption of ultrasound.
(3) Ultrasound stimulates the redistribution and dissolution of carbon, which was formerly in the form of graphite. In deeper and cooler layers, the influence of ultrasound compensates the weakening of the redistribution mechanism of diffusion.

References

[1] Amulevicius A, Balciuniene M, Petretis B and Pileckis R 1994 *Thin Solid Films* **240** 60
[2] Amulevicius A, Balciuniene M, Davidonis R, Kanapenas R, Reksnis J, Tamoliunas J and Jakstas E 1990 *Lith. J. Phys.* **30** 448
[3] Amulevicius A, Balciuniene M, Petretis B and Pileckis R 1993 *Thin Solid Films* **229** 192
[4] Abramov O V 1972 *Crystallization of Metals in Ultrasound Field* (Moscow: Metalurgija) p 256 (in Russian)
[5] Abramov O V *et al* 1986 *Influence of Powerful Ultrasound on Interphasic Surface of Metals* (Moskow: Nauka) p 278 (in Russian)
[6] Gureev D M 1998 *Fiz. Khim. Obrab. Mater.* **1** 73
[7] Jakstas E and Kanapenas R 1989 USSR patent specification 4648316/31-02
[8] Amulevicius A, Balciuniene M, Grigaliunas S and Petretis B 1993 *Fiz. Met. Metalloved* **76** 94
[9] Grigorianec A G 1989 *Principles of Laser Processing of Materials in Mechanical Engineering* p 304 (in Russian)
[10] Dubiel S M and Zinn W 1982 *J. Magn. Magn. Mater.* **28** 261
[11] Amulevicius A, Davidonis R, Kanapenas R, Reksnis J, Tamoliunas J and Jakstas E 1989 *Lith. J. Phys. 29* 494
[12] Dubiel S M and Zinn W 1984 *J. Magn. Magn. Mater.* **45** 298
[13] Lauermannova J 1973 *Proc. 5th Inter. Conf. on Mössbauer Spectroscopy (Bratislava)* Part 2, p 302
[14] Dubiel S 1976 *Acta Phys. Pol.* A **49** 619
[15] Grigorev I S and Meilihanov E Z (eds) 1991 *Tables of Physical Values Handbook* (Moskow: Energoatomizdat) p 1232 (in Russian)
[16] Ubbelohde A R 1978 *The Molten State of Matter* (London: Wiley) p 376
[17] Ficukov M M and Kosuskin V G 1996 *Fiz. Khim. Obrab. Mater.* **4** 122
[18] Bauer P, Uwakweh O N C and Genin J M R 1988 *Hyperfine Interact.* **41** 555
[19] Chekin V V 1982 *Mössbauer Spectroscopy of Iron, Tin and Gold* (Moscow: Energija) p 107 (in Russian)
[20] Brusilovskij V A and Geller A L 1997 *Fiz. Met. Metalloved* **83** 591
[21] Amulevicius A, Daugvila A, Davidonis R and Sipavicius C 1998 *Fiz. Met. Metalloved* **85** 1111
[22] Kraposhin V S, Iljin A I, Baranov V J and Sebrant A 1984 *Preprint* IAE-3917/9 (Moscow)
[23] Le Caer G and Bauer-Grosse E 1989 *Hyperfine Interact.* **47** 55